Full Paper Wiley Online Library ELECTROANALYSIS

DOI: 10.1002/elan.201600596

Mechanism of Chicoric Acid Electrochemical Oxidation and Identification of Oxidation Products by Liquid Chromatography and Mass Spectrometry

Emad F. Newair,*[a] Refat Abdel-Hamid,[a] and Paul A. Kilmartin[b]

Abstract: Electrochemical oxidation of chicoric acid (ChA) was investigated using cyclic voltammetry and chronoamperometry at a glassy carbon electrode. Chicoric acid generates single quasi-reversible redox wave in cyclic voltammetry over a wide pH range, and an ECEC-dimerization mechanism is proposed. Effect of glutathione (GSH) on the electrochemical oxidation of chicoric acid (ChA) was investigated in Britton–Robinson buffer solution. Ultra-high performance liquid chromatography (UPLC) coupled with mass spectrometry (MS) was used to show that the naturally occurring chicoric acid (ChA) underwent an electrochemical oxidation in the presence of glutathione (GSH) to form mono-, bi-, tri-, and four-glutathione conjugates of chicoric acid and a mono-glutathione conjugate of a chicoric acid dimer. The obtained results are useful for understanding and predicting the oxidative degradation pathway of chicoric acid.

Keywords: Cyclic voltammetry · Electrolysis · Oxidation Mechanism · Chicoric acid · Glutathione conjugates

1 Introduction

Medicinal herbs composed of *Echinacea* roots have become extremely popular in the United States as well as in Europe [1,2]. The main phenolics reported in *Echinacea* are phenolic acids and flavonol-glycosides. Chicoric acid (ChA, Figure 1) is the main phenolic in *Echinacea* roots [3]. ChA is generally used as a marker to evaluate the quality of herbal products [4]. ChA inhibits the production of free radicals and lipid peroxidation involved in the inflammation development [5]. It was also reported that ChA has potential antioxidant, anti-inflammatory, antiviral and immune-stimulating properties [6]. The antiviral activity of chicoric acid and its tetra-acetyl esters against HIV-1 was reported by Pluymers et al., [7]. Tousch et al. reported that ChA increases glucose uptake in L6 muscular cells by enhancing insulin release and glucose uptake [8]. ChA has immunostimulatory properties, protect the free radical-induced degradation of collagen and anti-hyaluronidase activity [6]. Kour and Bani demonstrated that ChA has a protective effect on chronic restraint stress [9]. Recently, ChA has been shown to have anti-cancer, anti-obesity, and anti-diabetic properties [10]. A significant reduction in acute alcohol-induced steatosis was observed on oral intake of chicoric acid in mice through interfering with inducible nitric oxide synthase (iNOS) in the liver [11].

ChA is a phenolic compound that belongs to the group of hydroxycinnamic acids containing two caffeoyl units (Figure 1). These two caffeoyl moieties can be oxidized electrochemically. It is worth mentioning that electrochemistry is a promising method for antioxidant properties investigation, and numerous reports are found in the literature concerning the application of electrochemical techniques to characterize polyphenolic compounds [12–20]. As a result it is well worthwhile to investigate the electrochemical behaviour of chicoric acid.

Generally, it has been found that the electro-oxidation of hydroxycinnamic acid derivatives with a catechol groupinvolves the transfer of two electrons coupled with two protons following a two-step ECEC mechanism. An unstable phenoxyl radical (semiquinone) intermediate is formed on transfer of one electron through the first step. It decays yielding a corresponding *o*-quinone as a final product in the second step [19,21]. It was reported by Sánchez et al. [22] that caffeic acid related derivatives, two dimeric amides and two dimeric esters, are electrochemically oxidized involving the catechol group via two-step mechanism. Investigation of the electrochemical oxidation mechanisms of verbascoside and rosmarinic acid, caffeic acid esters with two catechol moieties, was reported by Gil et al. [23]. The electrochemical oxidation mechanism of three dimeric and one tripodal as well as a monomeric benzylic esters, ferulic acid derivatives, were investigated [24]. The esters are oxidised electrochemically following an ECE mechanism.

The current study is concerned with an investigation of the electron transfer properties of chicoric acid (ChA) using cyclic voltammetry at a glassy carbon electrode,

[a] E. F. Newair, R. Abdel-Hamid
Unit of Electrochemistry Applications (UEA), Department of Chemistry, Faculty of Science, University of Sohag, Sohag 82524, Egypt
*e-mail: emad.newair@science.sohag.edu.eg
newair.emad@gmail.com

[b] P. A. Kilmartin
School of Chemical Sciences, University of Auckland
Private Bag 92019, Auckland, New Zealand

which is reported here for the first time. The study deals with the electrochemical behavior of ChA and attempts to elucidate the structures of intermediate species generated during the oxidative process. For this purpose, an electrochemical cell coupled with LC–MS constitutes an interesting tool to investigate the oxidative degradation of ChA, and provides information concerning the active redox sites of ChA as well as possible adduct reactions useful to determine the non-enzymatic degradation pathways.

2 Materials and Methods

2.1 Chemicals

Chicoric Acid (≥95% HPLC), rosmarinic acid (≥97.0%), L-glutathione reduced (≥98.0%), boric acid (≥99.5% ACS), glacial acetic acid (USP), phosphoric acid solution (49–51% HPLC), sodium hydroxide (≥98% reagent grade) were purchased from Sigma-Aldrich (France). Ethanol (≥99.8% HPLC) was obtained from Merck (United States). Alumina powder was obtained from Metrohm (France). All solutions were prepared using purified water from a Millipore (Milli-Q) system.

2.2 Solutions and Sample Preparation

The stock solution of ChA (1.78 mmol L^{-1}) was prepared in an ethanol/water (50:50) mixture. Britton–Robinson (B-R) buffer was used over the pH range from 1.80 to 8.80. B-R buffer consists of a mixture of phosphoric acid (0.04 mol L^{-1}), boric acid (0.04 mol L^{-1}) and acetic acid (0.04 mol L^{-1}) that has been titrated to the desired pH with ammonium hydroxide (0.2 mol L^{-1}).

The prepared solutions were kept in refrigerator and were protected from light with aluminum foil. Fresh solutions were prepared from the stock solutions by dilution for each new experiment.

2.3 Instruments

Autolab PGSTAT128N Potentiostat/Galvanostat (Eco-Chemie, Utrecht, The Netherlands) coupled with NOVA2.0 software was used for performing the electrochemical measurements on a standard 20 mL three-electrodes electrochemical cell. A glassy carbon electrode (GCE, $d = 3.0$ mm, model 61204300, Metrohm-Autolab, Switzerland), silver/silver chloride (Ag/AgCl, aq. KCl, 3.0 M) and platinum wire as working, reference and auxiliary electrodes were used, respectively.

The GCE surface was cleaned by polishing before each measurement with 0.3 μm alumina powder, then thoroughly rinsed with Milli-Q water and passed to the ultrasonic bath for 5 min. After mechanical polishing, the GCE was subjected to further electrochemical cleaning by cyclic voltammetry in B-R buffer supporting electrolyte to steady-state. All measurements were undertaken in duplicate.

The electrolysis reaction cell (μ-PrepCell, Antec, USA) contained a HyREF reference electrode (Pd/H_2), titanium counter electrode and a glassy carbon working electrode (1.9 cm^2). A bench-top pH-meter (HI 2210, HANNA Instruments, Romania) with a combined pH reference electrode was used for pH solution measurements. Millipore (Milli-Q) system was used for purification of water.

2.4 Electrolysis

For the electrochemical oxidation, ChA was dissolved to reach a concentration of 0.1 mM in an ethanol/water solution (50:50, v:v). The 0.1 mM solution of ChA was continuously passed at a flow rate of 0.1 mL/min through the electrochemical cell while a 300 mV was continually applied between the working electrode and the Pd/H_2 reference electrode. The potential was kept constant for more than 3 min to allow baseline stabilization, and then samples were collected in dyed vials under argon atmosphere for LC–MS analysis. A 5.0 mM glutathione solution was used to trap oxidized species.

2.5 UPLC-DAD-MS System

Chicoric acid and glutathione conjugates of chicoric acid have been identified using ultra-high performance liquid chromatograph coupled with mass spectrometer. An Acquity UPLC (Waters, Milford, MA) equipped with a photodiode array detector was used for the liquid chromatographic analysis. HSS T3, 100×2.1 mm, 1.8 mm column, Nucleosil 120-3 C18 end capped (Macherey-Nagel,Sweden), was used. The gradient conditions were as follows: solvent A (H_2O-HCOOH, 99/1, v/v), solvent B (CH_3CN-H_2O-HCOOH, 80/19/1, v/v/v); initial 0.1% B, a linear change to 60% B occurred from 0–5 min; then to 99% B from 5–7 min; 99% B isocratic. The Acquity UPLC system was coupled online with a mass spectrometer of amaZon X ESI-Trap (Bruker Daltonics, Bremen, Germany). For analysis, the applied coditions are: the nebulizer pressure was 44 psi, the dry gas temperature was set at 200 °C with a flow rate of 12 L min^{-1} and the capillary voltage was set at 4 kV. The mass spectral data were acquired over a 90–1500 Th mass range in the negative ionization mode. At 8.1m/z min^{-1}, the mass spectrum acquisition speed was set.

3 Results and Discussion

The electrochemical oxidation of phenolic acids is related to their free hydroxyl functional groups. They are oxidized initially to the unstable *o*-semiquinone radical and may undergo further reactions, such as coupling, proton loss or coupling of nucleophiles. Chicoric acid (ChA) possesses two caffeoyl moieties (i.e., four hydroxyl groups) which can be oxidized electrochemically.

3.1 Cyclic Voltammetry of Chicoric Acid

In order to deduce the electrochemical oxidation mechanism of chicoric acid (ChA), cyclic voltammetric behavior of 4.45×10^{-5} M ChA was investigated in aqueous Britton–Robinson buffer (pH 1.80) at GCE at scan rate (υ) of 20 mV s^{-1} (Figure 2A, black curve). ChA shows well-defined voltammetric waves, with an oxidation peak potential (E_p^a) of 540 mV, and a reduction peak potential (E_p^c) of 499 mV. The separation of peak potential $\Delta E_p = (E_p^a - E_p^c)$ was found to be 41 mV, which is a little larger than the value expected for a fully reversible system with two electrons (of 59/*n* mV) [25]. Furthermore, the peak ratio (i_p^c/i_p^a) was less than unity. These data indicate that the redox processof ChA at a GCE was apparently quasi-reversible. ChA has two catecholmoieties, which might be expected to show separate anodic waves, if the moieties are in different chemical environment. In fact, only one cyclic voltammogram peak was obtained, consistent with the two catechol groups being in the same chemical environment. It is well known that electrochemical oxidation of the 3,4-dihydroxymoiety shows a single anodic CV wave involving two electrons and two protons [23]. Therefore, the oxidation of ChA consumes four electrons and four protons. According to Faraday's law of electrolysis, the number of electrons (n) per oxidized molecule is given by n = Q/FN where, Q is charge passed in electrolysis, F is the Faraday's constant, and N is the number of mol. Bulk electrolysis with coulometric analysis was undertaken on 5.5×10^{-10} mol ChA in Britton–Robinson buffer (pH 1.80) at 300 mV vs. Pd/H_2. The net charge consumed was 1.99×10^{-4} Coulomb for 5.5×10^{-10} mol of ChA which corresponds to 3.8 electrons per molecule for the whole redox process.

For confirmation of the above mechanism, cyclic voltammetry of a related compound, rosmarinic acid (RA), was undertaken. Structurally, RA consists of caffeic acid (CAF) with 3,4-dihydroxyphenyl lactic acid (DHPLA) (Figure 1), while ChA consists of two caffeic acid moieties with tartaric acid. Both RA and ChA contain two catechol moieties. The two catechol moieties in RA one corresponds to CAF and the other to DHPLA, while in ChA they are related to CAF. The voltammetric behavior of 2.56×10^{-5} M rosmarinic acid was also tested in a B-R buffer solution (pH 1.80) at a GCE (Figure 2A, red curve). The oxidation of RA shows two distinguishable current steps, the first step appeared as a shoulder (peak 1a) at $E_p^{a1} = +0.486$ V, followed by an anodic peak 2a at $E_p^{a2} = +0.535$ V. The ΔE values for the two waves were 28 and 31 mV, pointing to a two-electron reversible electrode reaction. Development of the two distinguishable current steps is due to the substituent electron density and inductive effects, taking into account that ester and carboxylic groups have an electron-withdrawing effect (−I), while alkyl groups have an electron-releasing effect (+I). The electrostatic induction decreases along the conjugated chain, so the negative inductive effect of the carboxylic function in case of DHPLA will be small. On the other hand, the deactivating effect of the carboxyl function in the case of CA is kept by double bond [34–36], but the electron density in the phenolic groups of CA is decreased by the carboxylic group, making the electron transfer more difficult.

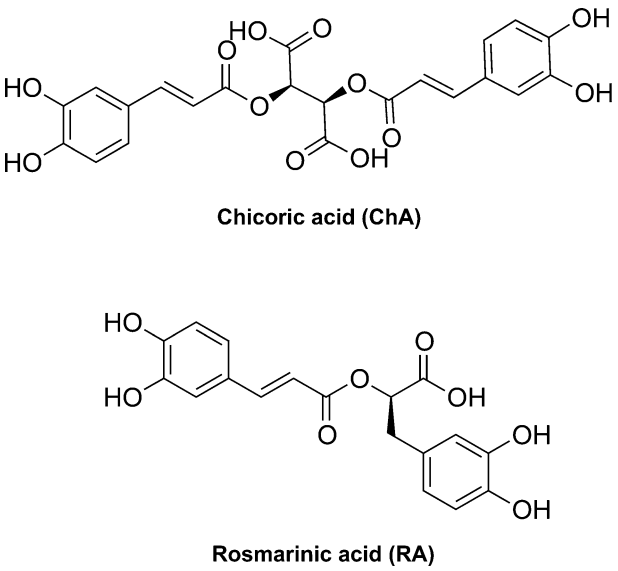

Fig. 1. The chemical structures of chicoric acid (ChA) and rosmarinic acid (RA).

3.1.1 Effect of Scan Rate

Cyclic voltammetric behaviour of 4.45×10^{-5} M ChA was studied at different scan rates, as shown in Figure 2B. On plotting the log–log relation, (log i_p (A) vs. log υ (V s^{-1}) for the oxidation and reduction waves, a linear relationship was obtained with gradients of 0.78 and 0.80, respectively (Figure 2C). This reveals that the peak current is due to both diffusion- (0.5 value expected) and adsorption- (value of 1.0 for pure adsorption) control processes.

The oxidation peak potential (E_p^a) of ChA also varies with scan rate. On increasing scan rate, the peak potential is shifted to more anodic values. On plotting the E_p^a–log ν relationship, a straight line was obtained with a slope ($\delta E_p/\delta \log \nu$) of 36.50 mV dec^{-1}. The relation can be expressed using the following equation (1):

$$E_p(V) = 0.0365 \log \nu\ (V\,s^{-1}) + 0.589,\ r = 0.980 \qquad (1)$$

This shows that the CV wave was due to an electron transfer process coupled with a chemical reaction. Furthermore, a decrease of i_p^c/i_p^a and a slight change of current function ($i_p/Cv^{1/2}$) on increasing scan rate were obtained. This suggests that the electrode reaction follows an electron transfer – follow up chemical reaction mechanism [29]. Generally, it is proposed that the electron transfer step of caffeic acid derivatives leads to the formation of *o*-semiquinone radical. This product may involve in further chemical reactions (coupling, proton loss

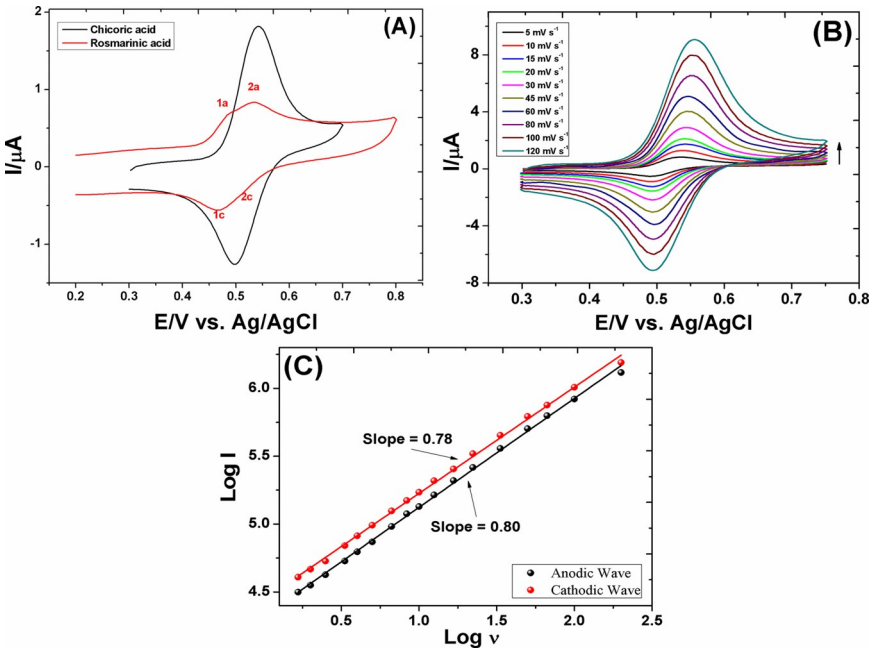

Fig. 2. (A) Cyclic voltammograms of 4.45×10^{-5} M chicoric acid (ChA) and 2.56×10^{-5} M rosmarinic acid in Britton–Robinson buffer (pH 1.80) at a GCE at a scan rate of 20 mV s^{-1}; (B) Cyclic voltammograms of 4.45×10^{-5} M chicoric acid (ChA) at a GCE in Britton–Robinson buffer (pH 1.80) at different scan rates; and (C) Log i_p vs. Log υ for ChA.

or nucleophilic attack) and finally may go for further electron transfer [30].

3.1.2 *Effect of pH*

Cyclic voltammograms of 2.63×10^{-5} M ChA solutions at scan rate of 20 mV s^{-1} on GCE in B–R buffer at different pH values from 1.80 up to 8.80 are performed and the results are shown in Figure 3A. The dependence of the peak potential (E_p) on pH provides valuable information concerning the electrode process. On increasing the solution pH, the anodic peak potential shifted linearly to less positive values, as shown in Figure 3B. Furthermore, the wave decreased and began to diminish at pH 7.33 and completely disappeared at a pH value greater than 8.8. These results indicate that the concentration of the electroactive form of chicoric acid ($ChAH_4$) is higher at acidic than basic pH values. On increasing solution pH, the concentration of $ChAH_4$ form was decreased consequently. The cathodic and anodic peak potentials shifted to more negative values. Figure 3B displays the average variation of the anodic and cathodic peak potentials for the ChA oxidation with pH at the GC electrode. This midpoint potential could be considered approximately as the conditional formal potential ($E^{\circ\prime}$). On plotting $E^{\circ\prime}$as a function of pH, a linear decrease of $E^{\circ\prime}$ value with a slope of −55.2 mV/pH, r = 0.995 was obtained (Figure 3B). The obtained relation is obeyed the following equation (2):

$$E^{\circ\prime} = E^{\circ} - 2.303\ (mRT/nF)\ pH \qquad (2)$$

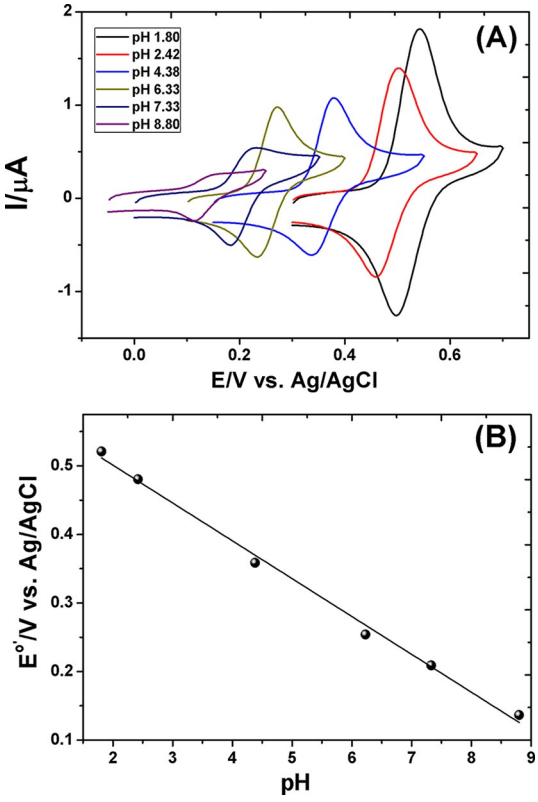

Fig. 3. (A) Cyclic voltammograms of 2.63×10^{-5} M chicoric acid (CHA) on bare GCE in Britton–Robinson buffer at a scan rate of 20 mV s^{-1} at different pH of 1.80, 2.42, 4.38, 6.33, 7.33 and 8.80; (B) $E^{\circ\prime}$(midway potential) vs. pH relationship.

where, m and n are the proton and electron numbers in the redox reaction, respectively. R is the gas constant and

T is the absolute temperature. Based on the relation between $E^{\circ\prime}$ and pH, the standard redox potential E° was obtained from the intercept ($E^{\circ} = 0.620$ V). The slope value obtained is close to that expected for a system with an equal number of electrons and protons, and is indicative of an ECEC mechanism [30]. The peak current ratio (i_p^c/i_p^a) of near unity is a criterion for the stability of *o*-semiquinone radical under the experimental conditions, whereas a value of i_p^c/i_p^a lower than unity, is related to a dimerization reaction [31]. ChA has been shown that the i_p^c/i_p^a value was lower than unity and decreased with increasing the pH of the solution. This indicates that there is an increase in the coupling reaction rate (probably dimerisation) of the anion formed from the deprotonation.

3.1.3 Effect of Concentration

The voltammetric behavior of ChA was studied in aqueous B–R buffer (pH 1.80) at scan rate of 20 mV s^{-1} at different ChA concentrations from 1.80×10^{-6} to 1.91×10^{-4} M (Figure 4). The anodic peak current (i_p^a) increased and the peak current ratio (i_p^c/i_p^a) decreased on increasing the ChA concentrations from 1.80×10^{-6} to 7.5×10^{-5} M. This indicates that the increase of i_p^a is attributed to both adsorption of ChA on the electrode surface and at the same time to enhancement of the oxidative dimerization reaction. On further increase in ChA concentration, a decrease in the linear variation of i_p^a with concentration was

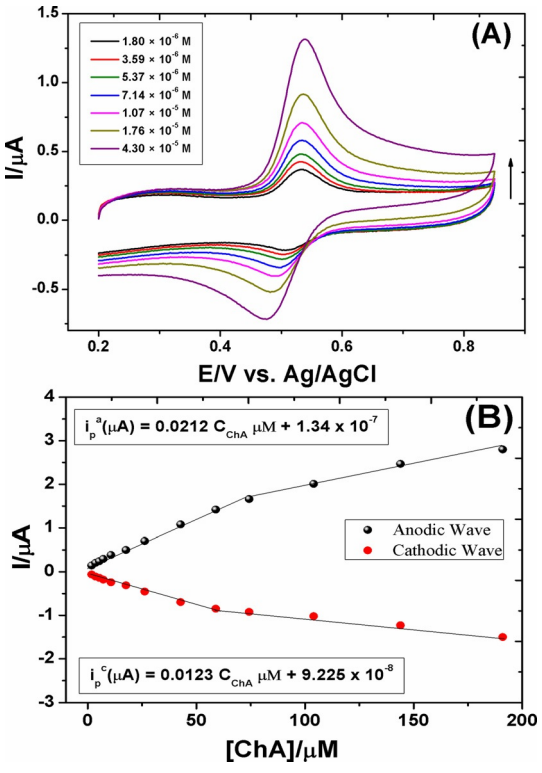

Fig. 4. Cyclic voltammograms of chicoric acid (CHA) on bare GCE in Britton–Robinson buffer (pH 1.80) at a scan rate of 20 mV s^{-1} at different ChA concentrations from 1.80×10–^{6} to 1.91×10^{-4} M. Inset: i_p vs. [ChA] relationship.

detected (no leveling off). This is ascribed to a complete coverage of the electrode surface, no contribution of the adsorption to i_p^a increase, while at the same time enhancing the oxidation reaction to dimerization.

3.2 Double Potential Step Chronoamperometry

For the determination of diffusion coefficient of the starting material (ChA), double potential step chronoamperometry was used. It can be estimated from the current data at first step i(t > τ), in which the magnitude of the chronoamperometric current of the first step depends on the D_S value, while that of the second step is controlled by both D_S and D_P values (D_S and D_P are diffusion coefficients for the starting and the product materials, respectively [32]. The chronoamperograms of 4.45×10^{-5} M ChA at a GCE in Britton–Robinson buffer (pH 1.80) were obtained using different duration times (data not shown). The diffusion coefficient can be estimated from the current data at first step i(t > τ) which is unaffected by the chemical reaction. Under diffusion, the current related to the electrode reaction of an electroactive substance is given by the Cottrell equation (3) [25]:

$$i(t < \tau) = nFAD^{1/2}\, C^*_{bulk}\, \pi^{-1/2}\, t^{-1/2} \qquad (3)$$

where D, C^*_{bulk}, and τ are diffusion coefficient (cm^2 s^{-1}), bulk concentration (mol L^{-1}) and step duration time, respectively and n, F, and A have their usual meaning. On plotting i(t < τ) versus $t^{-1/2}$, a straight line is obtained. The D value is estimated from the slope to be 6.93×10^{-5} cm^2 s^{-1}. The results also showed that there was a diffusional part to the oxidation of ChA over the entire time period and confirmed the above diffusion-adsorption controlled process.

3.3 Electrochemical Oxidation of Chicoric Acid (ChA) in the Presence of Glutathione (GSH) and Characterization of Oxidation Products Utilizing Ultra-high Performance Liquid Chromatography Coupled with Mass Spectrometry

3.3.1 Cyclic Voltammetry of Chicoric Acid (ChA) in the Presence of Glutathione (GSH)

The electrochemical oxidation of glutathione (GSH) to give the disulphide form of glutathione (GSSG) takes place through the loss of 2 protons and 2 electrons at a glassy carbon electrode. The electrode reaction has been reported as follows [15]:

$$2GSH \rightarrow GSSH + 2H^+ + 2e^-$$

Addition of glutathione solution to ChA solution showed a quite remarkable change in the cyclic voltammograms. When an excess amount of GSH was added to the ChA solution, an increase in the height of the oxidation peak and a significant decrease in the magnitude of the reduction peak were observed (Figure 5). These

changes are attributed to an electrocatalytic oxidation reaction of thiols with *o*-quinones, i.e, a rapid interaction of ChA quinone with the glutathione. Two potential electrochemical reactions can be presented as follows [15]:

1. GSH undergoes an electrochemical reduction of the formed quinone backward to the chicoric acid accompanied by the conversion of glutathione to the disulfide form (equation 4):
2. GSH interaction with the formed quinone to give a glutathione conjugate of chicoric acid (equation 5):

The output of these two mechanisms is the production of phenolic species (ChA itself and glutathione derivatives of ChA) that can be further oxidized at the glassy carbon electrode. The formation of this new phenolic species explains the observed increment in the anodic peak and decline in cathodic peak seen for cyclic voltammograms of a mixture of ChA with GSH. The influence of GSH on cyclic voltammograms of ChA at different pH values is presented in Figure 5. The cyclic voltammograms of GSH addition to ChA illustrates that the degree of reversibility of the ChA oxidation peak at around 550 mV was different for the various pH values. For example, Figure 5C shows that the cyclic voltammogram of 0.05 mM ChA with GSH at pH 8.8 was largely irreversible, pointing to a very rapid interaction between GSH and the formed ChA quinone leaving nothing available for reduction at the GC electrode on the reverse potential scan. Nevertheless, a cyclic voltammogram of 0.05 mM ChA with the same concentration of GSH at pH 1.8 and pH 4.38 still retained a cathodic peak (Figure 5A and 5B). The interaction rate between GSH and ChA quinone can be evaluated by adding different concentrations of GSH to the ChA solution. The anodic peak current (I_a) was proportional to the quantity of ChA ready to be oxidized to a quinone form, while the cathodic peak current (I_c) was proportional to the quantity of quinone ready to be reduced back to ChA. The decrease in the ratio I_c/I_a after GSH addition, compared to that ratio before GSH addition, was accordingly taken as an indication of the degree of interaction between GSH and quinone during the running experiment (Figure 5D). At pH 8.80, the initial concentration of ChA is decreased due to the dissociation process and the concentration of the oxidized products are decreased consequently. This indicates that ChA quinone interacted rapidly with GSH at pH 8.80. Cyclic voltammogram of 0.05 mM ChA with 0.15 mM GSH at pH 8.8 was completely irreversible, indicating that all of the formed ChA quinone interacted very rapidly with GSH, and the I_c/I_a ratio decreased to a low value. These results illustrate that GSH has an excellent ability to stabilize ChA when exposed to oxidation. The I_c/I_a ratio declined the least with GSH addition at pH 1.80, meaning that the quinone of ChA had the smallest interaction with GSH. It can be concluded that

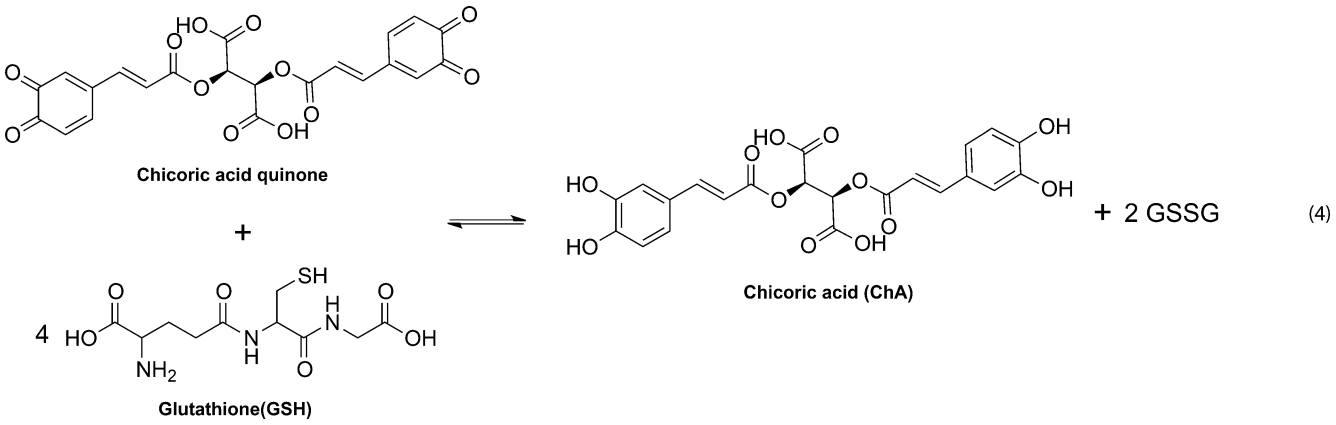

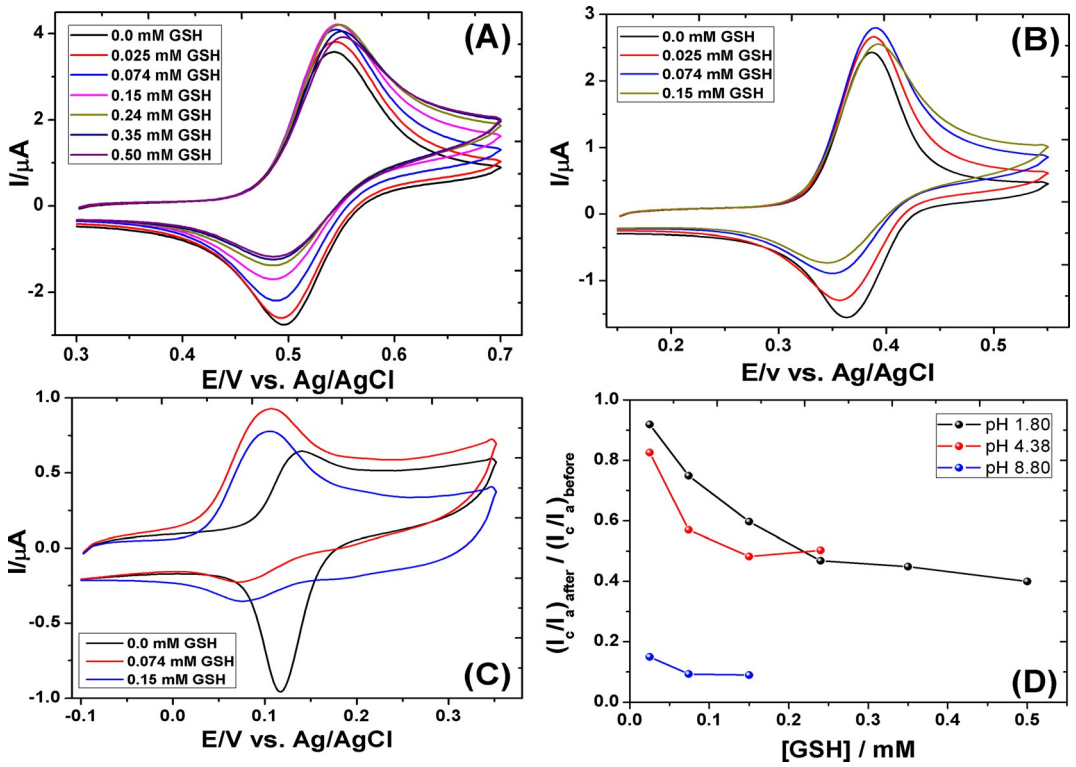

Fig. 5. Influence of glutathione on the cyclic voltammograms of 50.0 μM chicoric acid (ChA) on a bare GCE electrode in Britton–Robinson buffer at a scan rate of 20 mV s^{-1} at (A) pH 1.80, (B) pH 4.38, (C) pH 8.80; and (D) ratio of cathodic to anodic peak current before and after GSH addition at different pH values.

GSH protects ChA against oxidation at different pH values with a variable level of protection. Characterization of oxidation products by utilizing ultra-high performance liquid chromatography (UPLC) coupled with mass spectrometry (MS) for the electrochemical oxidation of ChA in the presence of GSH was undertaken at three different pH values (1.80, 4.38 and 8.80). The following sections discuss the results gathered in pH value of 1.8, while the results obtained in pH 4.38 and 8.80 are exactly the same, given that there was no change in oxidation products of ChA with GSH generated by changing the solution pH.

3.3.2 Identification of Oxidation Products of Chicoric Acid (ChA) by Ultra-high Performance Liquid Chromatography (UPLC) Coupled with Mass Spectrometry (MS)

Additional experiments were carried out using a commercial coulometric cell coupled with LC–MS in order to examine the electrochemical oxidation behavior of ChA in the presence of GSH at pH 1.8. For this purpose, two methods were used; in the first method, the oxidized ChA passing through the electrochemical cell was directly collected in a 0.5 mM GSH solution avoiding the direct electrochemical oxidation of GSH. In the second method, ChA solution was added to an excess of GSH (0.5 mM) and passed through the electrolysis cell. So even if the GSH was directly oxidized at the electrode surface at 300 mV vs. Pd/H_2, the UPLC-MS data showed that a significant fraction of GSH remained in the reduced form after electrolysis and could react with quinone species [33]. In both methods, important amounts of adduct products were obtained. The electrolyzed solutions were then examined using (UPLC-MS in order to identify the main conjugated species produced in the presence of glutathione.

Examination of the electrolyzed solution shows no significant electrochemical oxidation of ChA was observed when the potential was fixed at 0 mV vs. Pd/H_2; only a *m/z* 473 $[M-H]^-$ was observed which is assigned to ChA (Figure 6, black curve, peak A). At 300 mV vs. Pd/H_2, a series of new products were detected after trapping the electrolyzed solution with GSH (method 1) (Figure 6, red curve). Three relevant signals observed at *m/z* 778 $[M-H]^-$(peak B) and at *m/z* 1083 $[M-H]^-$(peak C) correspond to mono- and bi-glutathione conjugates of ChA, respectively. The third signal at *m/z* 625 $[M-2H]^{2-}$ (peak D) is assigned to the mono-glutathione conjugate of a ChA dimer. However, LC-MS data showed that a significant signal of ChA (peak A) remained in the reduced form after electrolysis. This can be explained by the ChA remaining after the reaction and also due to glutathione interacting with ChA quinone by reducing it back to the original ChA (Equation 4).

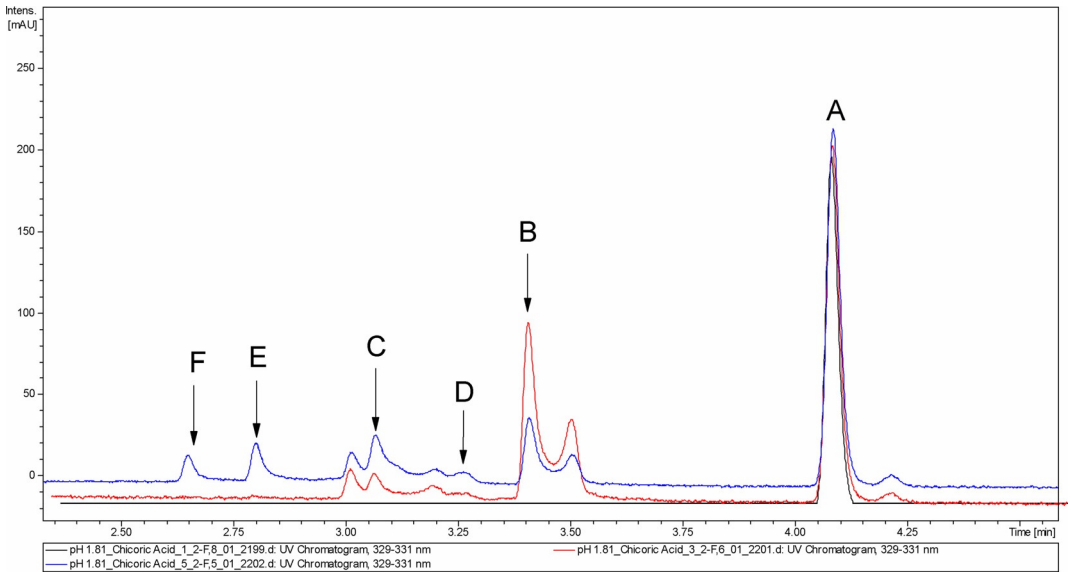

Fig. 6. UPLC–UV chromatograms at 330 nm of 50.0 μM chicoric acid (ChA) solution (black curve), 50.0 μM ChA solution oxidized at 300 mV vs. Pd/H_2 and trapped by a 0.5 mM GSH solution (red curve) and 50.0 μM ChA solution oxidized at 300 mV vs. Pd/H_2 in presence of 0.5 mM GSH solution. Mass to charge (*m*/*z*): 473 $[M-H]^-$ (A); 778 $[M-H]^-$ (B); 1083 $[M-H]^-$(C); 625 $[M-2H]^{2-}$ (D); 694 $[M-2H]^{2-}$ (E) and 847 $[M-2H]^{2-}$ (F).

The products of the electrochemical oxidation reaction of ChA in the existence of GSH were investigated by UPLC-MS. A fixed potential of 300 mV vs. Pd/H_2 was applied through B-R buffer solution of ChA with GSH for 5 min, and thereafter, these solutions were introduced onto the UPLC-MS unit. Two new peaks were observed on the UPLC chromatogram of the ChA–GSH mixture at 330 nm (peaks E and F, blue curve, Figure 6). Peak E at *m*/*z* 694 $[M-2H]^{2-}$corresponds the mass of a tri-glutathione conjugate of ChA. The predominant mass ion of peak F was at *m*/*z* 847 $[M-2H]^{2-}$, which corresponds to the four-glutathione conjugate of ChA. A similar mechanism was previously suggested to explain the presence of mono- and bi-glutathione conjugates for dihydroxycinnamic acids [34]. In another paper [35], the formation of mono-, bi- and tri-glutathione conjugates of catechin and mono-glutathione conjugate of catechin dimer were reported. Moreover, the four signals (peaks A, B, C and D) that appeared with method 1 were copletely the same peaks characterized during the electrochemical oxidation of ChA in the presence of GSH (method 2). Therefore, electrochemical oxidation of chicoric acid-glutathione mixture enhances the formation of tri- and four-glutathione conjugates of ChA. Considering all of the above observations, the electrochemical oxidation mechanisms of chicoric acid can be presented in Schemes 1 and 2.

The results described here demonstrate that ChA when oxidized electrochemically formed an *o*-quinone intermediate which readily formed glutathione conjugates of ChA. Mass spectrometry analysis identified mono-, bi-, tri- and four-glutathione conjugates of ChA and the mono-glutathione conjugates of a ChA dimer. It is worth noting that GSH could attack at all available positions on the formed *o*-quinone intermediate (Figure 7). The C5 and C2 of the ring are almost equally electrophilic reactive centers as they are adjacent to the carbonyl groups of the *o*-quinone, whereas the C6 is the least electrophilic center. However, what distinguishes between the three electrophilic centers is the steric hindrance in an increasing order C5 < C6 < C2. It is clear that the steric hindrance plays a major role as a distinguishing factor, and explains why glutathione attacks the C6 electrophilic center more readily than C2, despite the fact that C2 is more electrophilic than the C6 center. The C5 center is the most electrophilic and the least sterically hindered center [34]. The quinone of ChA is indeed a highly reactive species that can react with nucleophiles such as glutathione. In fact, glutathione is an important mechanism for cellular defense against reactive quinones [36].

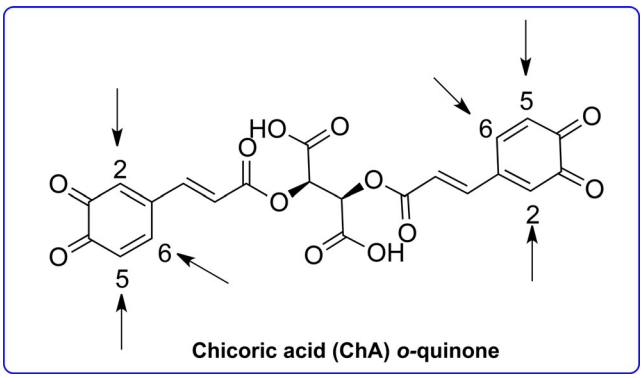

Fig. 7. Pattern for the glutathione conjugates formation of chicoric acid (ChA).

3.3.3 Proposed Mechanism of Chicoric Acid (ChA) Electrochemical Oxidation

The signals observed at *m/z* 778 $[M-H]^-$ (B); 1083 $[M-H]^-$ (C); 694 $[M-2H]^{2-}$ (E) and 847 $[M-2H]^{2-}$ (F) assigned to the mono-, bi-, tri- and four-glutathione conjugates of ChA, respectively. Based on these signals, the caffeoyl moiety of ChA would be induced by the abstraction of one electron-one proton leading to the formation of the radical species. The radical intermediate may also undergo a second electron-proton abstraction leading to the formation of the quinone. Taking in account the fact that GSH acts as a nucleophile and attacks reactive species such as quinones and that the GSH adduct species were obtained here at *m/z* 778 $[M-H]^-$ (B); 1083 $[M-H]^-$ (C); 694 $[M-2H]^{2-}$ (E) and 847 $[M-2H]^{2-}$ (F), an electrochemical oxidation pathway of ChA can be proposed, as displayed in Scheme 1.

The quinone formed after electrochemical oxidation of ChA (A) *m/z* 474 (method 1) undergoes a GSH addition reaction leading to the formation of mono- (B) and bi- (C) glutathione conjugates of ChA. On the other hand, the electrochemical oxidation of ChA in the presence of GSH (method 2), producing additional GSH adducts observed at *m/z* 694 $[M-2H]^{2-}$ and 847 $[M-2H]^{2-}$, indicates the development of tri- and four-glutathione conjugates of ChA (E and F, respectively).

Mass spectrometry analysis provided further evidence that the radical intermediate species could also undergo a dimerization reaction when oxidized electrochemically (Scheme 2). The signal D observed at *m/z* 625 $[M-2H]^{2-}$ assigned to the mono-glutathione conjugate of ChA dimer. It is worth mentioning that the ChA dimer is spontaneously oxidized at the electrode surface to produce the quinone of the ChA dimer. Furthermore, even by trapping the electrolyzed solution of ChA in GSH solution or by direct oxidation of ChA-GSH mixture, the ChA dimer undergoes GSH addition reaction to form the mono-glutathione conjugate of ChA dimer, as shown in Scheme 2.

4 Conclusions

This study has shown that the combination of electrochemical techniques with LC/MS may constitute a powerful tool for evaluating the oxidation behavior of chicoric acid. Possible electrochemical pathways were elucidated and different intermediate species were identified. The results show that chicoric acid electrochemically oxidizes via an ECEC radical–radical dimer mechanism using cyclic voltammetry and chronoamperometry. The use of electrochemical system combined with UPLC-MS was found to be useful for identifying possible adducts that are often difficult to identify from complex matrices. This

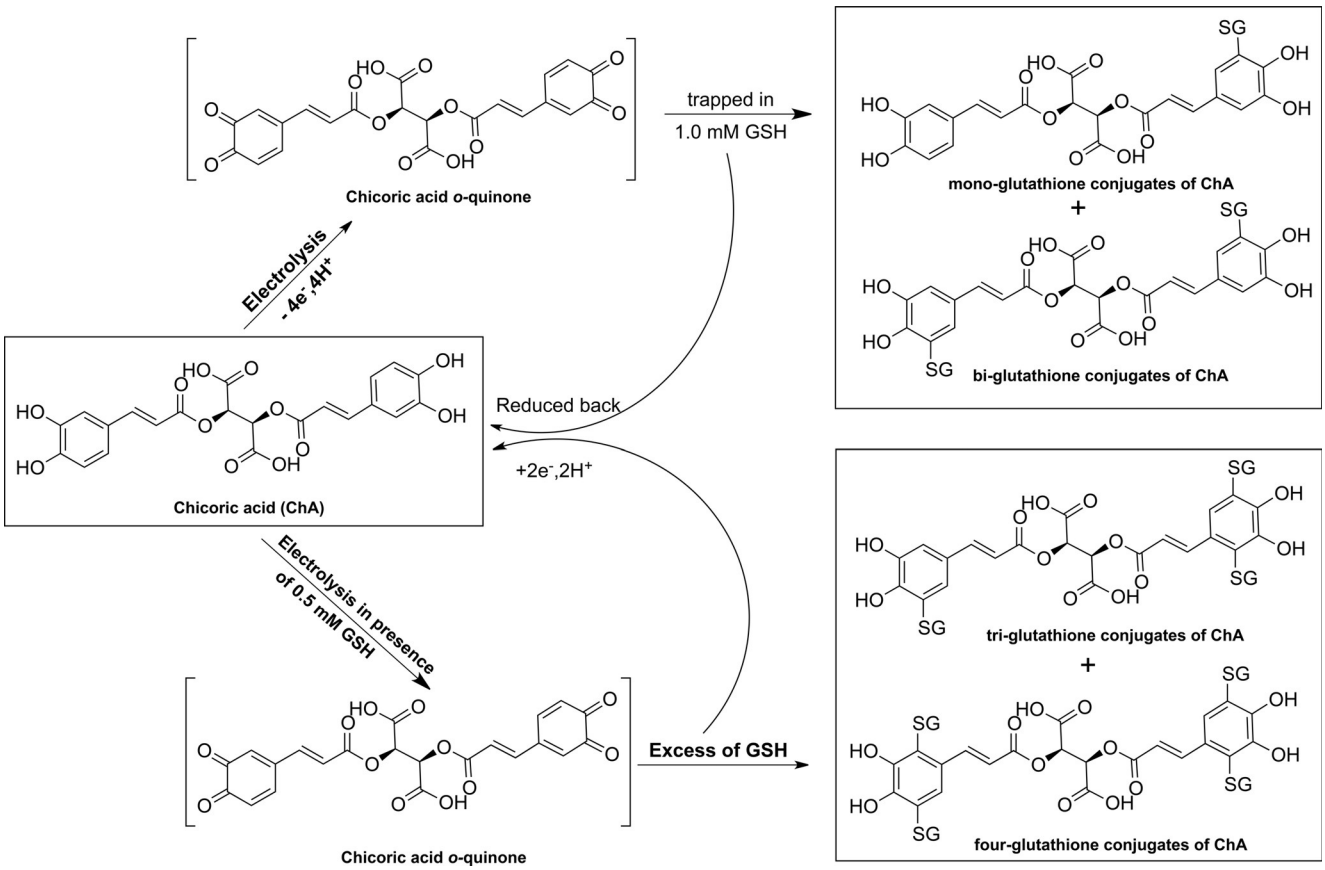

Scheme 1. Proposed pathway of the electrochemical formation of mono-, bi-, tri-, and four-glutathione conjugates of chicoric acid.

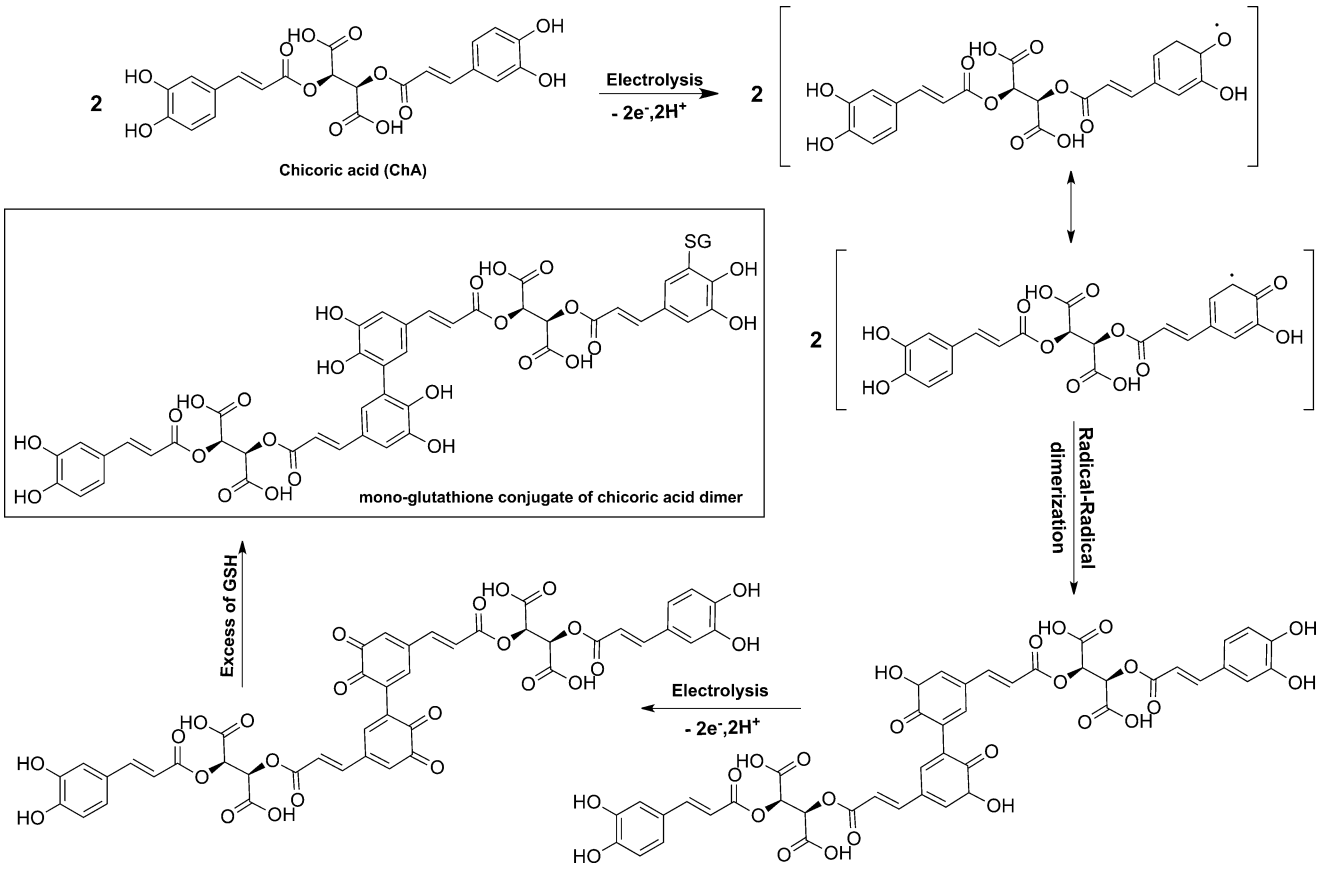

Scheme 2. Schematic pathway of the electrochemical synthesis of mono-glutathione conjugate of chicoric acid dimer.

technique (EC-UPLC-MS) may be utilized to estimate the action of additional antioxidants with polyphenols as well as to predict degradation pathways.

Acknowledgements

The authors gratefully acknowledge financial support from the Science and Technology Development Fund (STDF), Egypt, Grant No. (5361). Also, the authors thank, Dr. Hélène Fulcrand (Director of SPIRAL group) and Dr. François Garcia for useful discussion and technical training on UPLC-MS at UMR1083 Sciences Pour l'Oenologie (SPO), INRA-Supagro Montpellier Campus, France.

References

[1] R. Bauer, *Echinacea: Biological Effects and Active Principles. In L. D. Lawson, R. Bauer,* (Eds.), *Phytomedicines of Europe. Chemistry and Biological Activity*, American Chemical Society, Washington DC, **1998**, pp. 140–157.
[2] P. Brevoort, *HerbalGram* **1998**, 33–48.
[3] R. Bauer, *J. Herbs Spices Med. Plants* **1999**, *6*, 51–62.
[4] Y. Zhang, T. Tang, H. He, H. Wu, Z. Hu, *Ind. Crops Prod.* **2011**, *34*, 873–881.
[5] I. Stanisavljevic, S. Stajicevic, D. Velickovic, V. Veljkovic, M. Lazic, *Chinese J. Chem. Eng.* **2009**, *17*, 478–483.
[6] J. Barnes, L. A. Anderson, S. Gibbons, J. D. Philipson, *J. Pharm. & Pharmaco.* **2005**, *57*, 929–954 and references therein.
[7] W. I. M. Pluymers, N. Neamati, C. Pannecouque, V. Fikkert, C. Marchand, T. R. Burke, Y. V. E. S. Pommier, D. Schols, E. R. I. K. de Clercq, Z. Debyser, M. Witvrouw, *Mol. Pharmacol.* **2002**, *58*, 641–648.
[8] D. Tousch, A. D. Lajoix, E. Hosy, J. Azay-Milhau, K. Ferrare, C. Jahannault, G. Crosc, P. Petit, *Biochem. Biophys. Res. Commun.* **2008**, *377*, 131–135.
[9] K. Kour, S. Bani, *Neuropharmacol.* **2011**, *60*, 852–860.
[10] J. Lee, C. F. Scagel, *Front Chem.* **2013**, *1*, 1–40.
[11] M. Landmann, G. Kanuri, A. Spruss, C. Stahl, I. Bergheim, *Nutrition* **2014**, *30*, 882–889.
[12] P. A. Kilmartin, H. Zou, A. L. Waterhouse, *J. Agric. Food Chem.* **2001**, *49*, 1957–1965.
[13] S. K. Trabelsi, N. B. Tahar, B. Trabelsi, R. Abdelhedi, *J. Appl. Electrochem.* **2005**, *35*, 967–973
[14] R. Petrucci, P. Astolfi, L. Greci, O. Firuzi, L. Saso, G. Marrosu, *Electrochim. Acta* **2007**, *52*, 2461–2470
[15] O. Makhotkina, P. A. Kilmartin, *J. Electroanal. Chem.* **2009**, *633*, 165–174.
[16] O. Makhotkina, P. A. Kilmartin, *Anal. Chim. Acta* **2010**, *668*, 155–165.
[17] R. Abdel-Hamid, E. F. Newair, *J. Electroanal. Chem.* **2011**, *657*, 107–112.
[18] M. Salas-Reyes, J. Hernández, Z. Domínguez, F. González, P. D. Astudillo, R. E. Navarro, E. Martínez-Benavidez, C. Velázquez-Contreras, S. Cruz-Sánchez, *J. Braz. Chem. Soc.* **2011**, *22*, 693–701.

[19] R. Abdel-Hamid, M. K. Rabia, E. F. Newair, *J. Indian Chem. Soc.* **2013**, *90*, 463–467.
[20] O. Makhotkina, P. A. Kilmartin, *J. Agric. Food Chem.* **2013**, *61*, 5573–5581.
[21] C. Giacomelli, K. Ckless, D. Galato, F. S. Miranda and A. Spinelli, *J. Braz. Chem. Soc.* **2002**, *13*, 332–338.
[22] A. Sánchez, O. Martínez-Mora, E. Martínez-Benavidez, J. Hernández, Z. Domínguez, M. Salas-Reyes, *Org. Biomol. Chem.* **2014**, *12*, 5981–5989.
[23] E. de S. Gil, T. A. Enache, A. M. Oliveira-Brett, *Comb. Chem. High Throughput Screen* **2013**, *16*, 92–99.
[24] R. C. Guillén-Villar, Y. Vargas-Álvarez, R. Vargas, J. Garza, M. H. Matus, M.i Salas-Reyes, Z. Domínguez, *J. Electroanal. Chem.* **2015**, *740*, 95–104.
[25] A. J. Bard, L. R. Faulkner, *Electrochemical Methods, Fundamentals and Applications*, Wiley, New York, **2001**.
[26] M. Born, P. A. Carrupt, R. Zini, F. Bree, J. P. Tillement, K. Hostettmann, B. Testa, *Helv. Chim. Acta.* **1996**, *79*, 1147–1158.
[27] Y. Takahata, D. P. Chong, *Int. J. Quantum Chem.* **2005**, *103*, 509–515.
[28] E. S. Gil, C. H. Andrade, N. L. Barbosa, R. C. Braga, S. H. P. Serrano, *J. Braz. Chem. Soc.* **2012**, *23*, 565–572.
[29] R. S. Nicholson, I. Shain, *Anal. Chem.* **1964**, *36*, 706–723.
[30] H. Hotta, M. Ueda, S. Nagano, Y. Tsvjino, J. Koyama, *Anal. Biochem.* **2002**, *303*, 66–72.
[31] D. Nematollahi, M. Rafiee, *J. Electroanal. Chem.***2004**, *566*, 31–37.
[32] W. Hyk, A. Nowicka, Z. Stojek, *Anal. Chem.* **2002**, *74*, 149.
[33] U. Jurva, A. Holmén, G. Grönberg, C. Masimirembwa, L. Weidolf, *Chem Res Toxicol.* **2008**, *21*, 928–35.
[34] M. Y. Moridani, H. Scobie, A. Jamshidzadeh, P. Salehi, P. J. O'Brien, *Drug Metab. Dispos.* **2001**, *29*, 1432–1439.
[35] M. Y. Moridani, H. Scobie, P. Salehi, P. J. O'Brien, *Chem. Res. Toxicol.* **2001**, *14*, 841–848.
[36] P. J. O'Brien, *Chem. Biol. Interact.* **1991**, *80*, 1–41.

Received: September 17, 2016
Accepted: October 22, 2016
Published online: November 9, 2016

